

Machine learning quantification of lamellipodia in scanning electron microscopy (SEM) of Madin-Darby Canine Kidney Cells (MDCK)

Lucy Hui¹, Samar Micky², Mohamed Eisa², Angela Pearson², Amadou Barry¹

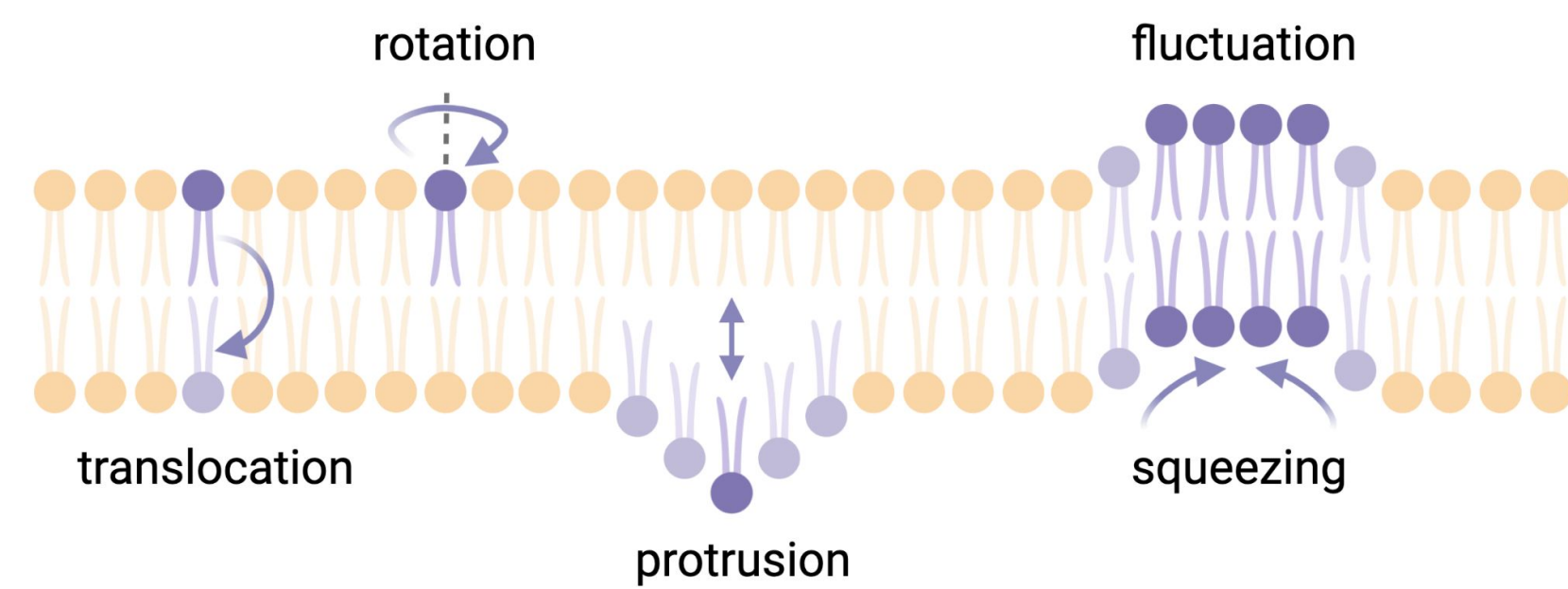
¹UMR INRS-UQAC en santé durable, Saguenay, Québec, Canada

²Centre Armand-Frappier Santé Biotechnologie, Institut National de la Recherche Scientifique, Laval, Québec, Canada

BACKGROUND

Membrane dynamics

- The dynamic nature of plasma membranes support many biological functions that are vital to cell survival [1].
- Variations in environmental factors such as pathogen exposure can alter membrane structures.



Membrane extensions

- Recent studies have revealed that viruses exploit membrane dynamics by inducing the formation of membrane protrusions, such as lamellipodia, in order to facilitate its entry, trafficking, and spread in host cells [2].
- Quantitative analysis of virus-induced changes in membrane structures represent an important avenue for studying viral pathogenesis and discovering treatment options.

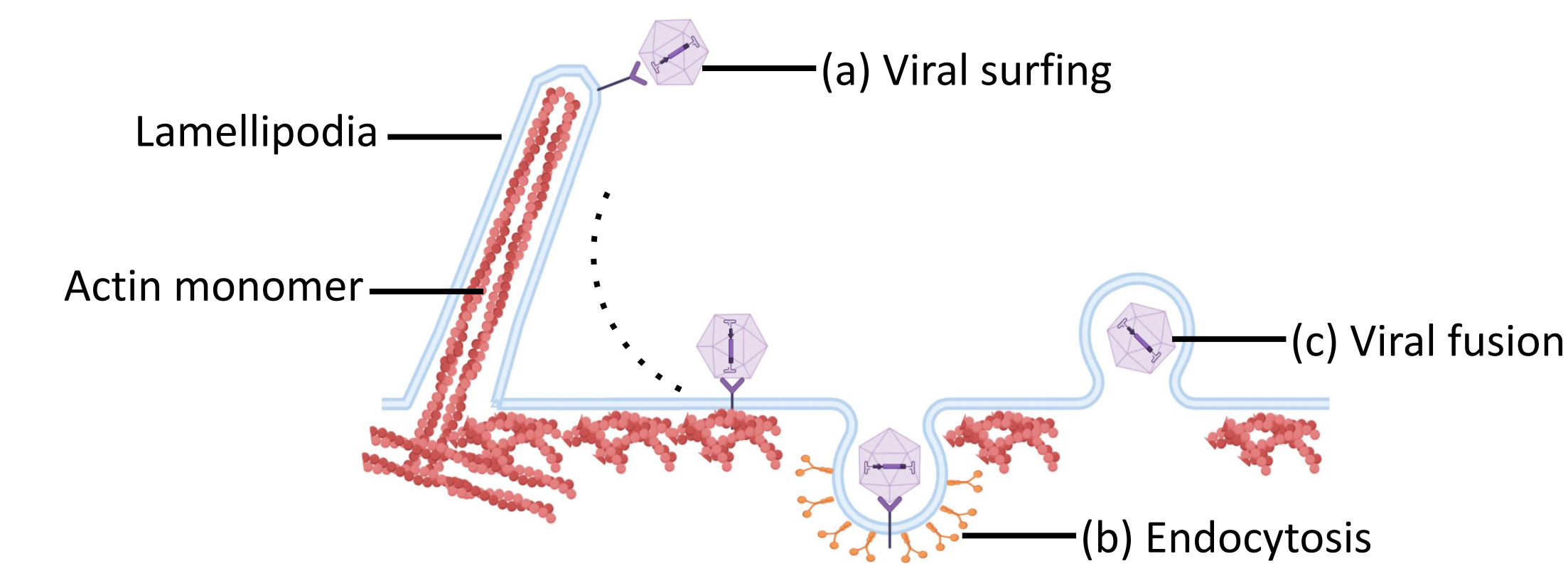


Figure 1. Modes of viral entry into host cell [3].

Study motivations

- Manual quantification of membrane extensions is time-consuming, inconsistent, and error-prone.
- Machine learning and deep learning pipelines for quantifying membrane extensions have not yet been established.

U-Net

- State-of-the-art and accessible deep learning model developed for biomedical image segmentation [5].

OBJECTIVES

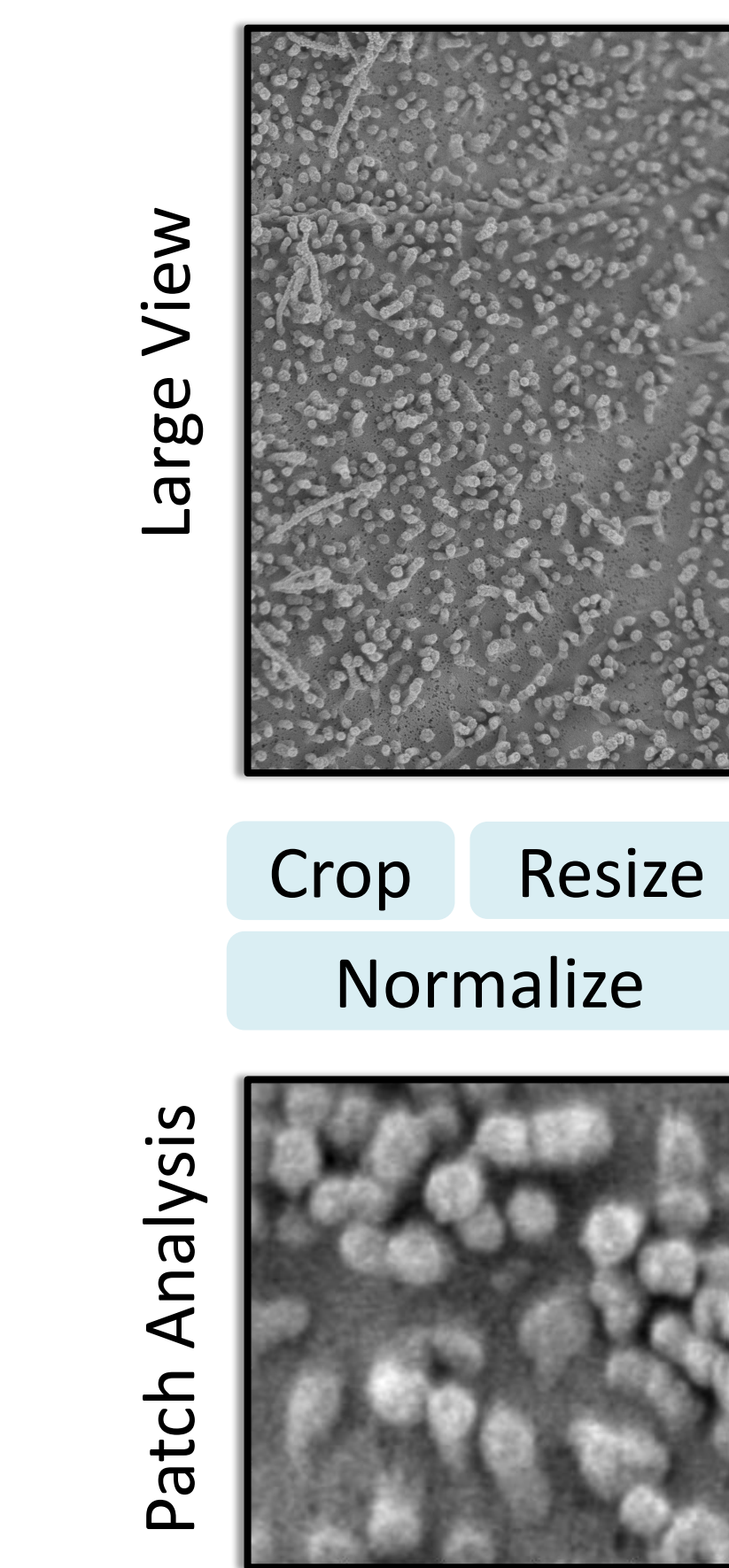
- Identify and apply diverse machine learning tools for quantifying lamellipodia in scanning electron microscopy (SEM) of MDCK.
- Evaluate and compare the performance of machine learning tools on lamellipodia detection and counting ability.
- Select and implement the best tools based on lamellipodia detection and counting ability.

REFERENCES

- A.C. Woodka, P.D. Butler, L. Porcar, B. Farago and M. Nagao. Lipid bilayers and membrane dynamics: Insight into thickness fluctuations. *Physical Review Letters*, DOI: 10.1103/PhysRevLett.109.058102, Vol. 9, Issue 5, Aug. 3, 2012.
- Eisa M, Micky S, Pearson A. Canid herpesvirus 1 Preferentially Infects Polarized Madin-Darby Canine Kidney Cells from the Basolateral Surface. *Viruses*. 2022 Jun 14;14(6):1291.
- Taylor M., Koyuncu, O. & Enquist, L. Subversion of the actin cytoskeleton during viral infection. *Nat Rev Microbiol* 9, 427–439 (2011).
- Faustino, G. M., Gattass, M., Rehen, S. & de Lucena, C. J. P. Automatic embryonic stem cells detection and counting method in fluorescence microscopy images. In 2009 IEEE International Symposium on Biomedical Imaging: From Nano to Macro, 799–802.
- N. Siddique, S. Paheding, C. P. Elkin and V. Devabhaktuni, "U-Net and Its Variants for Medical Image Segmentation: A Review of Theory and Applications," in *IEEE Access*, vol. 9, pp. 82031–82057, 2021.
- Eisa, Mohamed, et al. "Entry of the Varicellovirus Canid Herpesvirus 1 Into Madin-Darby Canine Kidney Epithelial Cells Is pH-Independent and Occurs via a Macropinocytosis-like

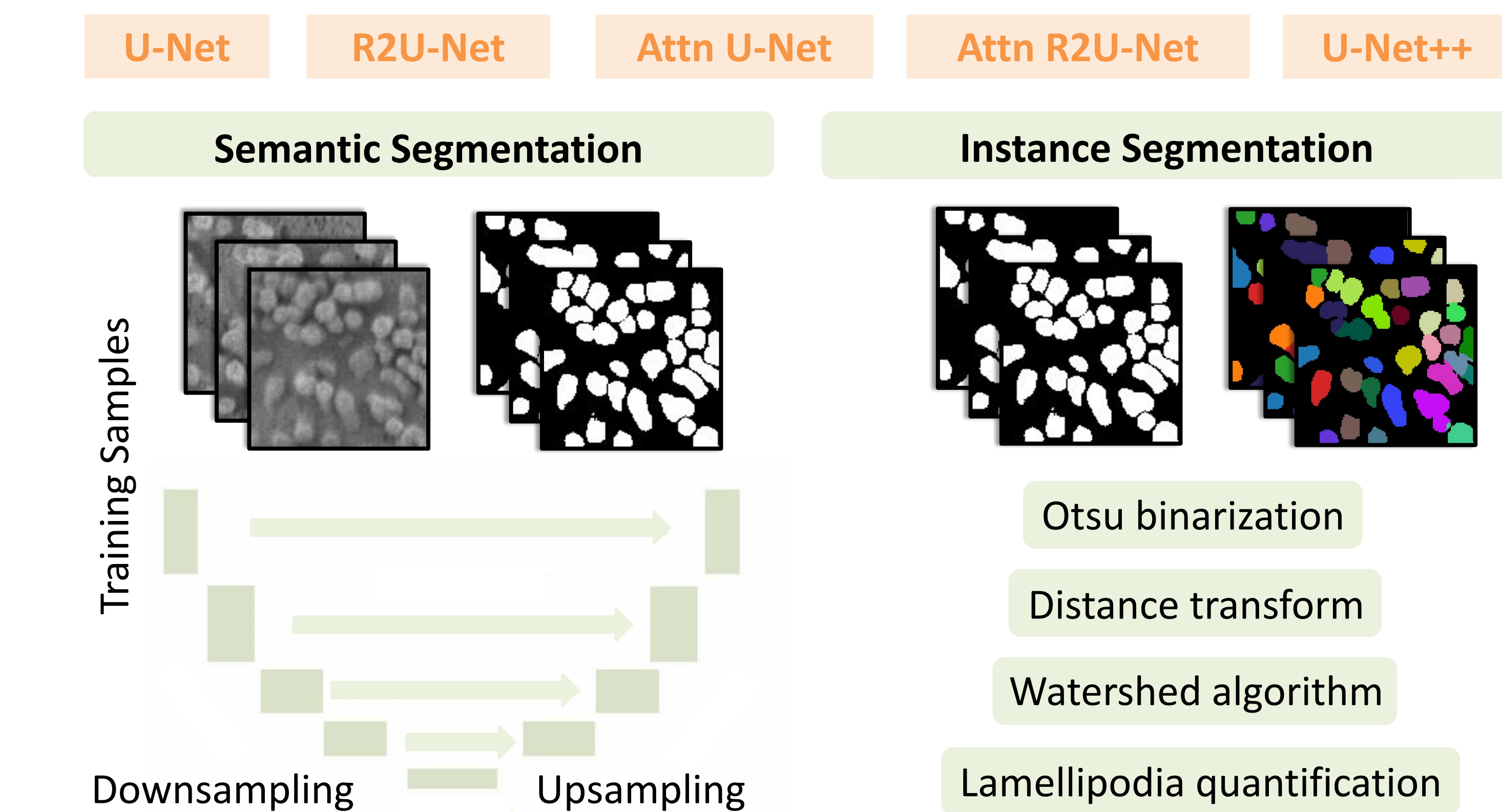
PIPELINE

Data pre-processing



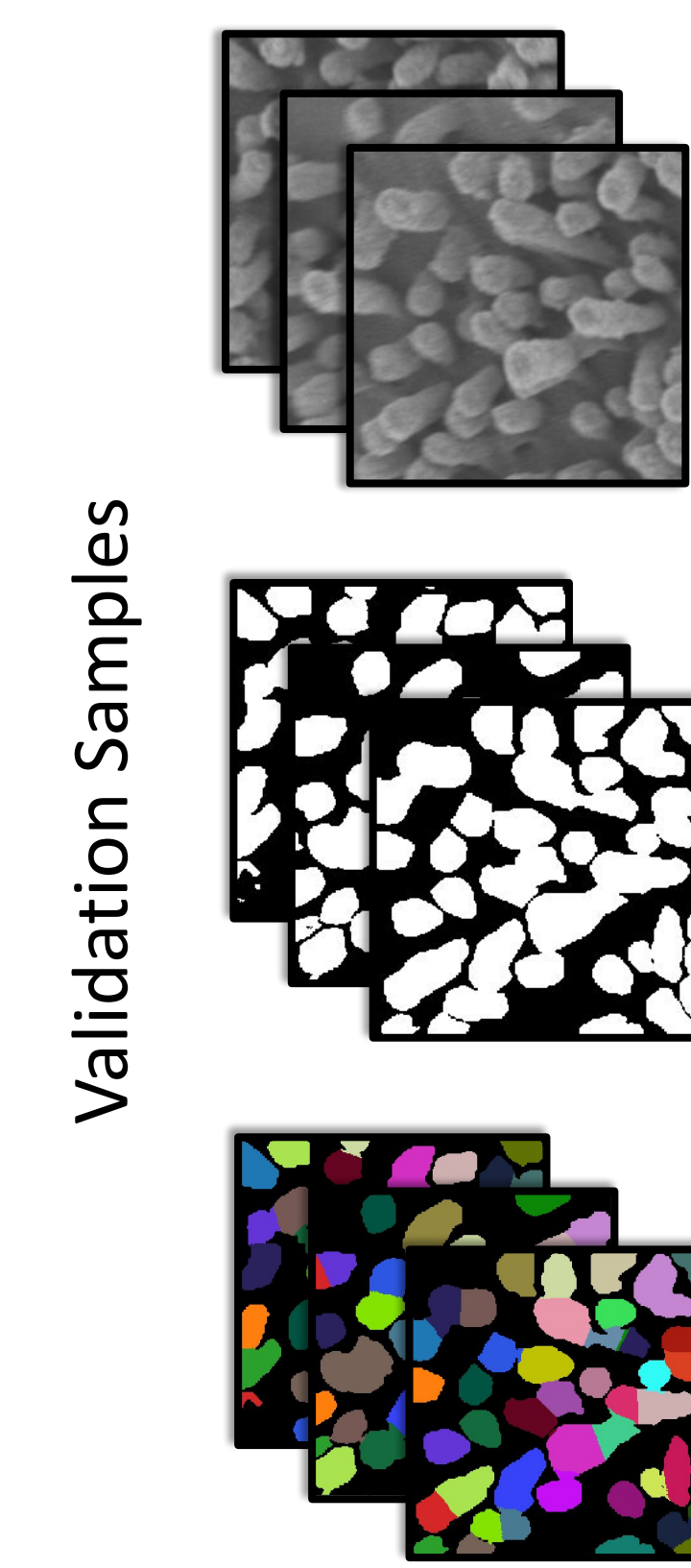
Model training

Apical surface of polarized MDCK cells grown on inserts [2]



Model evaluation

MDCK cells grown as monolayers on tissue culture plates [6]



Detection Metrics

$$\text{Accuracy} = (\text{TP} + \text{TN}) / (\text{TP} + \text{FP} + \text{FN})$$

$$\text{Precision} = \text{TP} / (\text{TP} + \text{FP})$$

$$\text{Recall} = \text{TP} / (\text{TP} + \text{FN})$$

$$\text{F1 score} = 2 * \text{TP} / (2 * \text{TP} + \text{FP} + \text{FN})$$

TP = true positive TN = true negative

FP = false positive FN = false negative

Quantification Metrics

$$\text{Mean Absolute Error} = \frac{1}{n} \sum_{i=1}^n |n_{\text{true}} - n_{\text{predict}}|$$

$$\text{Mean Percentage Error} = \frac{1}{n} \sum_{i=1}^n n_{\text{true}} - n_{\text{predict}} / n_{\text{true}}$$

RESULTS

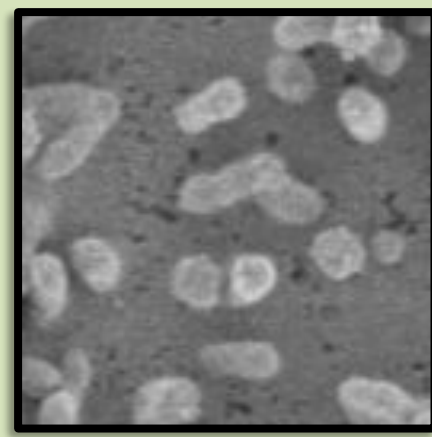



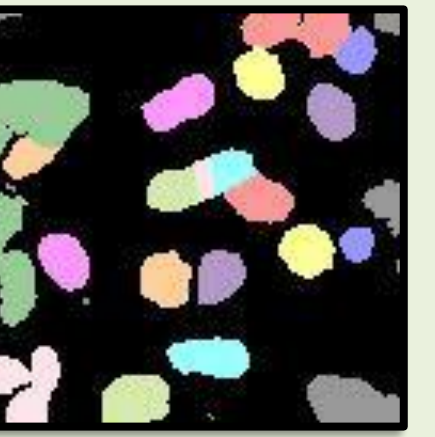


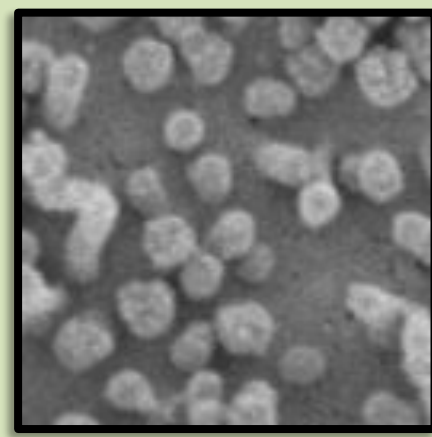
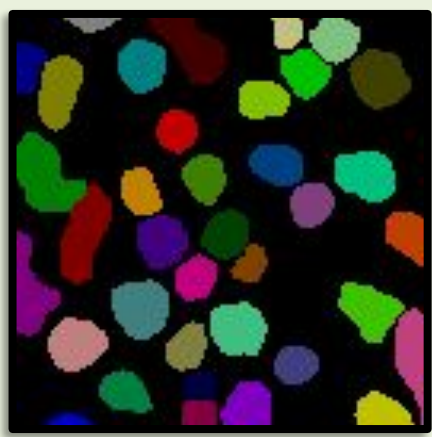





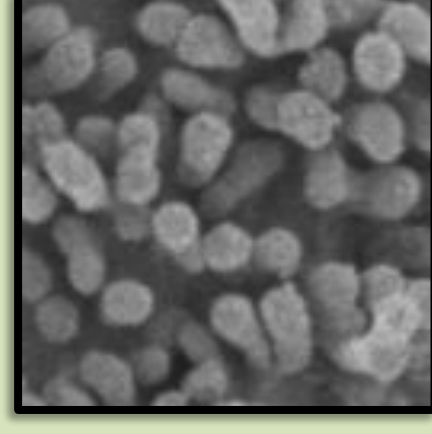






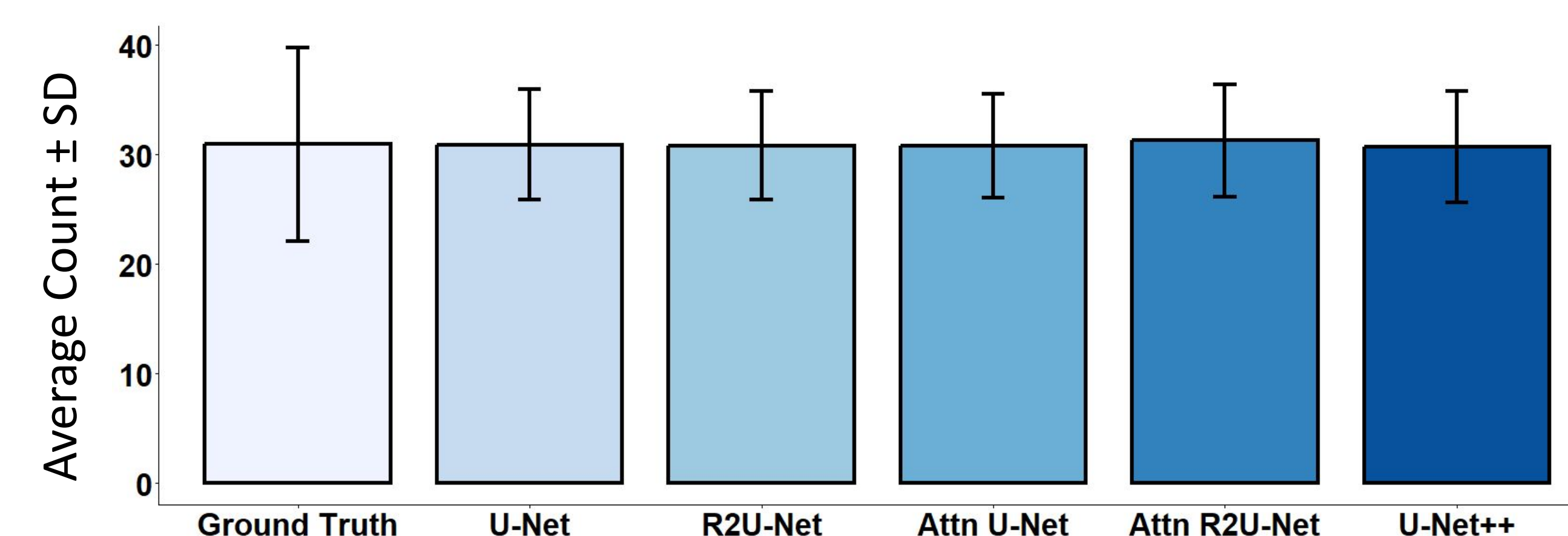
Original SEM	Ground Truth	U-Net	R2U-Net	Attn U-Net	Attn R2U-Net	U-Net++
	 Count: 20	 Count: 22	 Count: 21	 Count: 20	 Count: 23	 Count: 18
	 Count: 37	 Count: 32	 Count: 29	 Count: 30	 Count: 29	 Count: 29
	 Count: 41	 Count: 39	 Count: 38	 Count: 40	 Count: 39	 Count: 40

Table 1. Quantification of lamellipodia. Every unique color corresponds to one lamellipodia. Counts from machine learning methods (U-Net, R2U-Net, Attn U-Net, Attn R2U-Net, U-Net++) are comparable to manual count (Ground Truth) in three SEM images representing low, moderate, and high density.



Code availability



git lucy-mhui

METRICS

	Mean Accuracy	Mean Precision	Mean Recall	Mean F1	MAE	MPE (%)
U-Net	0.9383	0.9162	0.9348	0.9240	5.6	22.6
R2U-Net	0.9379	0.9110	0.9402	0.9238	5.2	21.5
Attn U-Net	0.9365	0.9182	0.9278	0.9212	5.6	22.9
Attn R2U-Net	0.9379	0.9092	0.9298	0.9238	5.3	21.7
U-Net++	0.9384	0.9229	0.9279	0.9239	5.1	20.9

Table 2. Evaluation metrics. U-Net++ surpassed other models on lamellipodia detection and quantification, however this difference is non-significant.

DISCUSSION

- We show the ability of U-Net architectures to segment, detect, and quantify lamellipodia from SEM images of MDCK cells.
- Average count from all five machine learning methods were comparable to average manual counts, however, counts from machine learning methods consistently had lower variability compared to manual counts.
- Automated counting of plasma membrane structures will increase researchers' ability to quantify changes to the plasma membrane ultrastructure in response to different environmental conditions.

ACKNOWLEDGEMENTS

INRS Centre Armand-Frappier Santé Biotechnologie Electron Microscopy Service